Stratigraphic Analysis of Phyllosilicate and Hydrated Sulfate Deposits Across the Margaritifer – Meridiani Boundary

J. B. Adler and J. F. Bell III
Arizona State University School of Earth and Space Exploration
(jacob.b.adler@asu.edu)

P41A
3889

1. Introduction

- Spectral signatures of aqueously altered minerals have been identified from orbit and at the surface (Opportunity rover) at Meridiani Planum and have been remotely identified at several potential landing sites in Margaritifer Terra [1-3]
- Phyllosilcate deposits are exposed on both sides of this regional boundary near Miyamoto Crater at different elevations and in different geologic units
- We present a regional geologic map and cross sections, which tie deposits at candidate landing sites [4-6] to a common geologic timeline

2. Methods

- CRISM [7] Multispectral Survey (MSP) and Full-Resolution Targeted (FRT) sequences in the mapped region (0-6°S, 3.5-10°W) were atmospherically corrected for CO_2 absorptions in ENVI with CRISM Analysis Tools software [8]
- A regional phyllosilicate strength map was constructed from a “survey mode” CRISM D2300 parameter mosaic [9]
- Reflectance spectra of high phyllosilicate signature regions are compared to the CRISM spectral library [10]
- Geologic map was created using JMARS and ArcMap software, THEMIS, CTX, and HiRISE images, MOLA and HRSC digital terrain models (DTMs) [11-17]
- Cross sections hypothesized relating candidate landing sites

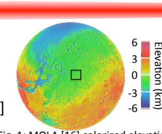

Fig. 1: MOLA [16] colorized elevation map marking extent of mapped region.

Fig. 3: (Right) Pixels in image MSP00004886_L with 2.3 micron band depth between 4 and 5% were spectrally averaged, ratioed to a background noise region, and continuum removed before comparison with the CRISM spectral library data.

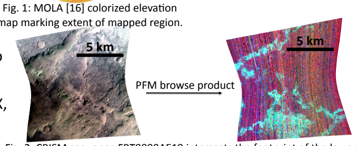

Fig. 2: CRISM sequence FRT0000AE19 intersects the footprint of the lower resolution MSP0004886 and exhibits Mg/Fe rich phyllosilicates (Smectite?) in cyan for the PFM browse product defined in Viviano et al 2014. [18]

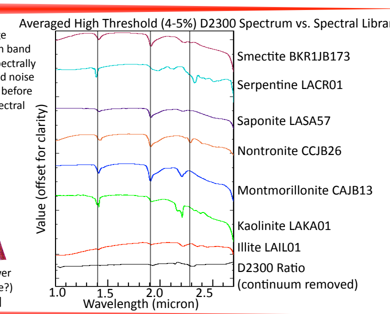

3. Results

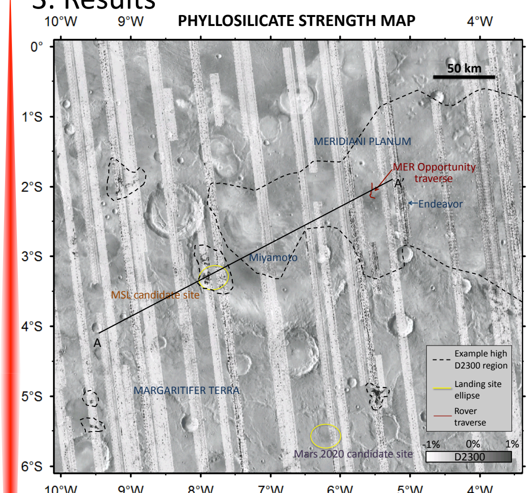

Fig. 4: Regional phyllosilicate strength map from mosaicked CRISM MSP strips (200m/pixel) over THEMIS Day IR.

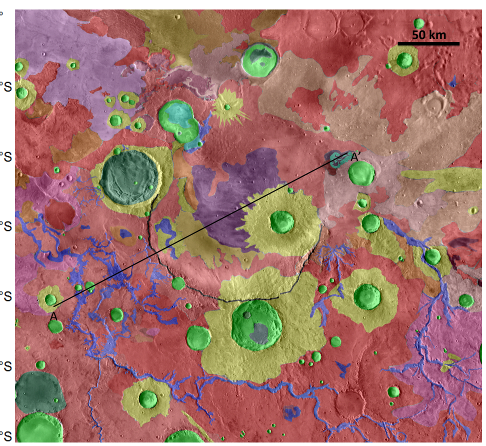

Fig. 5: Geologic map highlights morphological units with separate depositional and erosional processes. THEMIS night IR, CTX, and HiRISE images were used to follow contacts.

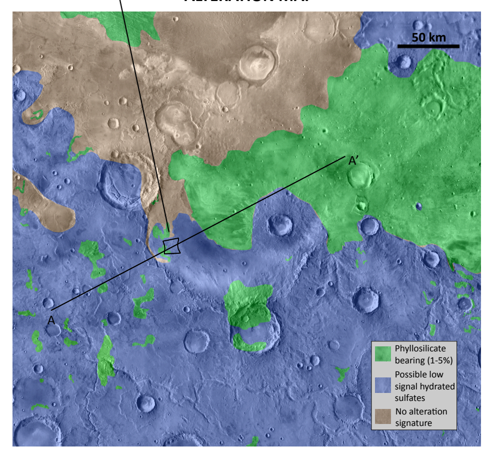

Fig. 6: Alteration map smooths phyllosilicate bearing units between survey mode coverage gaps by following associated THEMIS night IR (albedo, shade, texture) and CTX images (color, morphology).

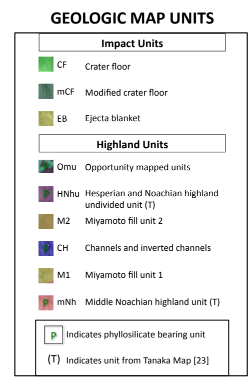

Fig. 7: Selected map units for reference with Figs. 5, 11.

- High resolution images were used to examine stratigraphic relations
- In all cases, surficial phyllosilicates had been exhumed from beneath one or more units

4. Consistency with Existing Maps


Fig. 8: Hynek & Di Achille 2014. [22]

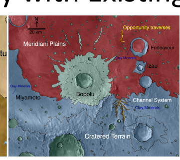
Fig. 9: Wiseman et al 2010. [20]

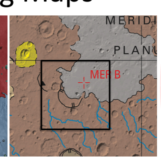

Fig. 10: Tanaka et al. 2014. [23]

5. Interpretations

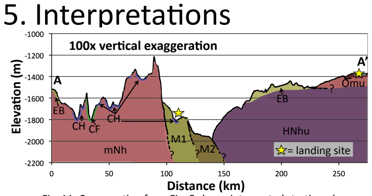

Fig. 11: Cross section from Fig. 5 shows interpreted stratigraphy

- Depositional sequence consistent with other local maps [5,19,20]
- Multiple episodes of aqueous activity, not necessarily consistent with global depositional event
- Most deposits exhumed from beneath thin capping layer (sedimentary/volcanic)
- Aeolian transport unlikely according to [24], this study more consistent with fluvial travel or in-situ formation

6. References

Cited: [1] Bibring J-P. et al. (2006) *Science*, 312, 400-403. [2] Squyres, S. W. et al. (2006) *JGR,* 111, E12S12. [3] Squyres, S. W. et al. (2004) *Science*, 306, 1698-1703. [4] Newsom H. E. et al. (2008) Presentation at 3rd MSL Landing Site Workshop, NASA, JPL. [5] Newsom H. E. et al. (2010) *Icarus,* 205, 64-72. [6] Christensen et al. (2014) Presentation at 1st M2020 Landing Site Workshop, Crystal City, VA. [7] Murchie S. et al. (2007) *JGR*, 112, E05S03. [8] Seelos F. (2012) Presentation at CRISM Data User’s Workshop, The Woodlands, TX. [9] Pelkey S. M. et al. (2007) *JGR,* 112, E08S14. [10] Seelos, F. (2009) Presentation at CRISM Data Users’ Workshop, The Woodlands, TX. [11] Christensen, P. R. et al. (2009) JMARS – A Planetary GIS, AGU. [12] ESRI (2011) ArcGIS Desktop: Release 10. Redlands, CA. [13] Christensen, P. R. et al. (2004) *Space Science Reviews*, 110, 85-130. [14] Malin M. C. et al. (2007) *JGR*, 112, E05S04. [15] McEwen, A. S. et al. (2007) *JGR*, 112, E05S02. [16] Smith D. E. et al (2001) *JGR,* 106, E10, 23,689-23,722. [17] Jaumann R. et al (2007) *PSS*, V55, 928-952. [18] Viviano-Beck, C. E. (2014) *JGR*, 119, 1403-1431. [19] Wiseman S. M. et al. (2008) GRL 35, L19204. [20] Wiseman S. M. et al. (2010) *JGR*, 115, E00D18. [21] Hynek, B. M. (2002), *JGR*, 107, E10 5088. [22] Hynek, B. M. & Di Achille, G. (2014) *LPSC*, 2193. [23] Tanaka, K. L. (2014) Geologic Map of Mars: USGS Scientific Investigations Map 3292. [24] Marzo G. A. et al. (2009) *GRL* 36 L11204. **See also:** Baldridge A. M. et al. (2009) GRL 36, L19201. Wray J. J. et al. (2009) GRL 36, L21201. **Acknowledgements:** Mark Salvatore, Nathan Williams.